Mon. Not. R. Astron. Soc. **358,** 572–584 (2005) doi:10.1111/j.1365-2966.2005.08804.x

The evolution of binary fractions in globular clusters

N. Ivanova,★ K. Belczynski,†‡ J. M. Fregeau and F. A. Rasio
Northwestern University, Department of Physics & Astronomy, Evanston, IL 60208, USA

Accepted 2005 January 5. Received 2004 December 27; in original form 2004 October 1

ABSTRACT

We study the evolution of binary stars in globular clusters using a new Monte Carlo approach combining a population synthesis code (STARTRACK) and a simple treatment of dynamical interactions in the dense cluster core using a new tool for computing three- and four-body interactions (FEWBODY). We find that the combination of stellar evolution and dynamical interactions (binary–single and binary–binary) leads to a rapid depletion of the binary population in the cluster core. The *maximum* binary fraction today in the core of a typical dense cluster such as 47 Tuc, assuming an initial binary fraction of 100 per cent, is only $\sim$5–10 per cent. We show that this is in good agreement with recent *Hubble Space Telescope* observations of close binaries in the core of 47 Tuc, provided that a realistic distribution of binary periods is used to interpret the results. Our findings also have important consequences for the dynamical modelling of globular clusters, suggesting that 'realistic models' should incorporate much larger initial binary fractions than has usually been the case in the past.

Key words: stellar dynamics – methods: *N*-body simulations – binaries: close – binaries: general – globular clusters: general – globular clusters: individual: NGC 104 (47 Tucanae).

1 INTRODUCTION

Binary stars play a fundamental role in the evolution of globular clusters for at least two important reasons. First, the evolution of stars in binaries, whether in a cluster or in the galactic field, can be very different from the evolution of the same stars in isolation. In a dense environment such as a globular cluster, this difference is exacerbated by dynamical encounters, which affect binaries much more than single stars. Secondly, binary stars crucially affect the dynamical evolution of globular clusters, providing (through inelastic collisions) the source of energy that supports them against gravothermal collapse (Goodman & Hut 1989; Gao et al. 1991; Fregeau et al. 2003). In the 'binary burning' phase, a cluster can remain in quasi-thermal equilibrium with nearly constant core density and velocity dispersion for many relaxation times, in a similar way to that in which a star can maintain itself in thermal equilibrium for many Kelvin–Helmholtz times by burning hydrogen in its core. The binary fraction[1] (and the initial, primordial binary fraction in particular), is therefore one of the most important parameters that determine the evolution of globular clusters. However, most previous dynamical studies of globular clusters – even those including binaries – have neglected stellar evolution, which can significantly impact the properties and survival of binaries and hence the reservoir of energy they provide.

At present, there are very few direct measurements of binary fractions in clusters. However, even early observations showed that binary fractions in globular cluster cores are smaller than in the solar neighbourhood (e.g. Cote et al. 1996). Recent *Hubble Space Telescope* (*HST*) observations have provided further constraints on the binary fractions in many globular clusters (Rubenstein & Bailyn 1997; Bellazzini et al. 2002b). The measured binary fractions in dense cluster cores are found to be *very small*. As an example, the upper limit on the core binary fraction of NGC 6397 is only 5–7 per cent (Cool & Bolton 2002). On the other hand, in very sparse clusters, such as NGC 288 (Bellazzini et al. 2002a), but also in some other 'core-collapsed' clusters, such as NGC 6752 (Rubenstein & Bailyn 1997), the upper limit for the binary fraction can be as high as $\sim$30 per cent.

For the *initial* binary fraction in globular clusters, there are of course no direct measurements. However, there are no observational or theoretical arguments suggesting that the formation of binaries and hierarchical multiples in dense stellar systems should be significantly different from other environments such as open clusters, the Galactic field, or star-forming regions. Binary frequencies $\gtrsim$50 per cent are found in the solar neighbourhood and in open clusters (Halbwachs et al. 2003). T Tauri stars also have a very high binary fraction (Köhler, Leinert & Zinnecker 2001). For the range of separations between 120 and 1800 au, their binary fraction is

★E-mail: nata@northwestern.edu
†Present address: New Mexico State University, Department of Astronomy, 1320 Frenger Mall, Las Cruces, New Mexico 88003-8001, USA.
‡Tombaugh Postdoctoral Fellow.

[1] Throughout this paper, the 'binary fraction' among a particular group of objects is defined as the number of objects that are binaries divided by the total number of objects. So, for example, a primordial binary fraction of 50 per cent implies that two-thirds of main-sequence stars are in binaries initially. However, a binary fraction of 50 per cent among white dwarfs (WDs) later on does not imply that two-thirds of white dwarfs are in binaries, as some white dwarf companions may be main-sequence stars.

comparable to that of main-sequence stars in the solar neighbourhood (Brandner et al. 1996), while at shorter periods it is higher (Melo 2003). Furthermore, many stars are formed in systems of multiplicity 3 or higher: in the field their abundance is no less than 40 per cent for inner periods $\leqslant$10 d (Tokovinin 1997). All of this suggests that, in dense stellar systems as well, most stars could be formed in binary and multiple configurations.

Most dynamical interactions in dense cluster cores tend to *destroy* binaries (the possible exception is tidal capture, which may form binaries, but turns out to play a negligible role; see Section 5.2). Soft binaries (with orbital speeds lower than the cluster velocity dispersion) can be disrupted easily by any strong encounter with another passing star or binary. Even hard binaries can be destroyed in resonant binary–binary encounters, which typically eject two single stars and leave only one binary remaining (Mikkola 1983), or produce physical stellar collisions and mergers (Bacon, Sigurdsson & Davies 1996; Fregeau et al. 2004).

In addition, many binary stellar evolution processes lead to disruptions [e.g. following a supernova (SN) explosion of one of the stars] or mergers (e.g. following a common envelope phase). These evolutionary destruction processes can also be enhanced by dynamics. For example, more common envelope systems form as a result of exchange interactions (Rasio, Pfahl & Rappaport 2000), and the orbital shrinkage and the development of high eccentricities through hardening encounters may lead to the coalescence of binary components (Hills 1984; Hurley & Shara 2003).

It is therefore natural to ask whether the small binary fractions measured in old globular clusters today result from these many destruction processes, and what the *initial binary fraction* must have been to explain the current numbers. We address these questions in this paper by performing calculations that combine binary star evolution with a treatment of dynamical interactions in dense cluster cores. In Section 3 we describe in detail the method we use, following a brief overview of the theoretical background in Section 2. We test our simplified dynamical model by comparing it against full Monte Carlo N-body simulations in Section 4.1. In Section 4.2 we use semi-analytical estimates to predict the upper limit for the final binary fraction in dense clusters. In Section 4.3 we estimate the lower limit for the final binary fraction and analyse which mechanisms of binary destruction are most efficient as a function of cluster age. In Section 5 we present our numerical results for the evolution of the binary fraction in dense cluster cores, and we compare these results with observations. In particular, using our theoretically predicted period distribution, we re-examine observations of 47 Tuc and re-derive constraints on the core binary fraction. In the final discussion (Section 6), we point out how our results may be helpful in interpreting observations of core binary fractions in other clusters, and we discuss the required initial conditions for simulations of clusters with binaries, and which methods are best suited for these simulations.

2 BINARY POPULATION SYNTHESIS WITH DYNAMICS

There are several possible ways to approach the study of binary evolution in dense clusters. The traditional approach is to start from full N-body simulations to study the dynamics of the stellar system and to introduce on top of this various simplified treatments of single and binary star evolution. This has been used for many years (for recent examples see Portegies Zwart et al. 2001; Shara & Hurley 2002; Hurley & Shara 2003). Unfortunately, even with the fastest special-purpose computers available today, this direct N-body approach remains extremely expensive computationally, so that previous studies have been limited to small systems such as open clusters and with limited coverage of parameter space. In addition, because binaries are particularly expensive to handle computationally (as they increase enormously the dynamic range of direct N-body simulations), these previous studies have also been performed with unrealistically small numbers of binaries. For example, the time required to perform just one direct N-body simulation of a cluster containing 2×10^5 stars with all stars formed initially in binaries would be at least a year on GRAPE-6, with some dependence on the initial binary parameters.[2]

Alternatively, a binary population synthesis code (e.g. Hurley, Tout & Pols 2002), normally used to evolve large numbers of stars and binaries without dynamical interactions, can be extended by introducing a simple treatment of dynamics. In this type of approach it is often assumed that all the relevant parameters of the cluster (e.g. central density and velocity dispersion) remain constant throughout each dynamical simulation, i.e. the dynamics is assumed to take place in a *fixed background* cluster. Many previous studies of dense stellar systems have been based on this type of approximation (see, e.g., Hut, McMillan & Romani 1992; Di Stefano & Rappaport 1994; Sigurdsson & Phinney 1995; Portegies Zwart et al. 1997a,b; Davies 1995; Davies & Benz 1995; Davies 1997; Rasio et al. 2000; Smith & Bonnell 2001). This approach, sometimes called the 'encounter rate technique' (Benacquista 2002), is computationally much less expensive than direct N-body simulations and hence allows the systematic exploration of the vast parameter space of initial conditions for clusters and their primordial binary populations. In addition, the use of sufficiently large numbers of stars and binaries makes the simulations more realistic. Although obviously much less accurate in its description of the overall cluster dynamics, this method opens the possibility of studying 'star cluster ecology' in considerably greater detail than has been possible with N-body simulations. In particular, it makes it possible to study in detail the rare but important evolutionary channels that may play a crucial role in the formation of some of the most interesting tracers of dynamical interactions in dense clusters, such as ultracompact X-ray binaries, millisecond pulsars and cataclysmic variables (Ivanova & Rasio 2004, 2005).

Unfortunately, it is difficult to compare these two approaches, as each is based on a very different set of simplifying assumptions. There are no comprehensive studies of dense stellar systems including a self-consistent treatment of both dynamics and binary star evolution. In many recent N-body simulations for large clusters (using either Aarseth-type codes or Hénon's Monte Carlo method; Aarseth 2001; Fregeau et al. 2003), binary stars are treated in the point-mass limit and soft binaries are eliminated from the start. Binary destruction can then occur only through resonant four-body interactions. However, N-body studies of open clusters that incorporate realistic treatments of binary stellar evolution have shown that stellar evolution affects the binaries significantly, and that, even in these low-density environments, the complex interplay between binary evolution and dynamics, even for soft binaries, can play an important role in the overall cluster evolution and in determining the properties of surviving binaries (Hurley & Shara 2003).

The second approach, 'binary population synthesis with dynamics', which we have adopted in this work, suffers from the lack of self-consistent dynamical evolution of the cluster, which is assumed

[2] J. Hurley, personal communication. The estimate is based on 5 d required to simulate an open cluster of 20 000 stars with 2000 binaries on GRAPE-6 in Shara & Hurley (2002).

to remain in a constant state of thermal equilibrium for its entire evolution. This state, where the energy production through 'binary burning' in the core is balanced by the outer energy flux into the cluster halo, does indeed provide nearly constant conditions throughout the lifetime of a typical globular cluster. The exception might be 'core-collapsed' clusters, which may have run out of binaries and evolved to a much more centrally concentrated state. Typically, the density and 'temperature' profiles of a cluster do not change much as long as there are enough binaries remaining to provide support against gravothermal contraction. Stellar interiors provide a useful analogy: as long as a star keeps enough hydrogen to burn in its core, it can remain in thermal equilibrium on the main sequence and avoid core contraction and envelope expansion. Just like main-sequence stars, globular clusters can maintain a nearly constant interior structure for many thermal time-scales (i.e. many relaxation times) as long as they do not run out of 'fuel' (binaries). This behaviour is expected qualitatively (see, e.g., Goodman & Hut 1989), and has now been demonstrated quantitatively in many different studies using various numerical techniques for cluster simulations. For example, the recent study by Fregeau et al. (2003) considered the evolution of idealized clusters of equal-mass stars without stellar evolution for a range of initial binary fractions. For the case of an isolated Plummer model with 10 per cent initial hard binaries they found (see their fig. 4) that the core radius of this cluster can remain nearly constant (to within a factor of ~ 2) for many tens of half-mass relaxation times (i.e. more than a Hubble time for most Galactic globular clusters, where the half-mass relaxation time is $\sim 10^9$ yr). For a more realistic cluster model with 20 per cent hard binaries initially and tidal truncation, they found that, after $\sim 40\,t_{\rm rh}$, when the cluster is about to disrupt in the Galactic tidal field, the core radius still has not varied by more than a factor ~ 2 over the entire evolution (see their fig. 11); and over the first $10\,t_{\rm rh}$, the core radius changed by less than ~ 20 per cent. The central velocity dispersion also does not vary much with time (see, e.g., Giersz & Spurzem 2003, fig. 1). Similar results have been obtained from direct N-body simulations of open clusters, where the central density and velocity dispersion also remain nearly constant in models with significant numbers of binaries (Hurley & Shara 2003).

There are several binary population synthesis codes in use today. Only a few of them include, in addition to a detailed treatment of mass transfer phases, stellar evolution along with tidal interaction of binary components. The code of Hurley et al. (2002) was designed to study low- and intermediate-mass stars leading to the formation of white dwarf systems. The code of Belczynski, Kalogera & Bulik (2002, Belczynski et al., in preparation) was originally developed to investigate more massive stars – progenitors of neutron star and black hole systems (calibrated against full binary stellar evolution codes for mass-transfer phases) – and was expanded recently to treat carefully binaries with white dwarfs as well. We use the latter code (called STARTRACK) to follow the evolution of single and binary stars in our simulations. As mentioned earlier, we also treat all dynamical encounters explicitly by direct integration, using a recently developed numerical toolkit for small-N gravitational dynamics that is particularly well suited to performing three- and four-body integrations (Fregeau et al. 2004).

3 METHODS AND ASSUMPTIONS

3.1 Cluster initial conditions

Our initial conditions are described by the following parameters: the total number of stars N (single or in a binary), initial mass function (IMF), binary fraction $f_{\rm b}$, distribution of binary parameters (period, P, eccentricity, e, and mass ratio, $q = m_2/m_1 < 1$). We typically adopt standard choices used in previous population synthesis studies, which are based on available observations for stars in the field and in young star clusters (Sills et al. 2003). For most of the calculations reported here, we use the following 'standard' initial conditions.

(i) We adopt the IMF of Kroupa (2002), which can be written as a broken power law $\mathrm{d}N \propto m^{-\alpha}\,\mathrm{d}m$, where $\alpha = 0.3$ for $m/\mathrm{M}_\odot < 0.08$, $\alpha = 1.3$ for $0.08 \leqslant m/\mathrm{M}_\odot < 0.5$, $\alpha = 2.3$ for $m/\mathrm{M}_\odot \geqslant 0.5$. We assume that all stars are formed in a single burst of star formation at $t = 0$ in our simulations.

(ii) We consider a wide range of stellar masses from 0.05 to 100 $\mathrm{M}_\odot$.[3]

(iii) The binary mass ratio, q, is assumed to be distributed uniformly in the range $0 < q < 1$. This is in agreement with observations for $q \gtrsim 0.2$ (Woitas, Leinert & Köhler 2001).

(iv) The binary period, P, is taken from a uniform distribution in $\log_{10} P$ over the range $P = 0.1$–10^7 d.

(v) The binary eccentricity, e, follows a thermal distribution with probability density $p(e) = 2e$.

(vi) We reject systems where binary components would overflow their Roche lobe at pericentre.

The initial average stellar mass is then $\langle m \rangle \simeq 0.5\ \mathrm{M}_\odot$, and, with the flat mass ratio distribution, the average binary mass is $\langle m_{\rm b} \rangle \simeq 0.75\ \mathrm{M}_\odot$.

3.2 Stellar evolution

We evolve all stars (single and binary) using the population synthesis code STARTRACK (Belczynski et al. 2002), which has recently been updated significantly (Belczynski et al., in preparation). This is the only current population synthesis code that incorporates detailed treatments of all possible types of mass transfer (MT) episodes: stable MT (conservative or non-conservative), unstable MT (thermally or dynamically) and thermal time-scale MT. Also included are the effects of Eddington-limited mass accretion and transient behaviour of accretion discs (based on the disc instability model). STARTRACK allows us to follow the evolution of binaries with a large range of stellar masses, metallicities and star formation histories (constant rate, sudden or exponential bursts, etc.). STARTRACK also models in detail the loss of mass and angular momentum through stellar winds (dependent on metallicity) and gravitational radiation, asymmetric core collapse events with a realistic spectrum of compact object masses, and the effects of magnetic braking and tidal circularization on close binaries. In our simulations, we adopted the new prescription for magnetic braking given by Ivanova & Taam (2003). Compared with the older prescription (Verbunt & Zwaan 1981) closer binaries lose their angular momentum at a slower rate and hence survive as binaries longer. The evolution of single stars in STARTRACK is based on the analytic fits provided by Hurley, Pols & Tout (2000), but includes a more realistic determination of compact object masses (Fryer & Kalogera 2001).

We treat the evolution of stellar collision and binary merger products following the general 'rejuvenation' prescription of Hurley et al. (2002). It ensures that the merger product has the same total amount of hydrogen, helium and carbon as the two parent stars together. For some stars, the assumptions made in the treatment of the merger

[3] The lower limit is chosen in order to provide a self-consistent mass-ratio distribution for binaries with primaries down to 0.15 $\mathrm{M}_\odot$.

depend on the types of stars and the type of merger (collision versus binary coalescence). For example, we assume that there is no accretion on to a neutron star during a physical collision, and that the other star, if it is unevolved, is destroyed completely (e.g. we do not consider the possible formation of a Thorne–Żhytkow object). We treat as a 'dynamical common envelope (CE)' event the outcome of a physical collision between a compact object and a red giant, applying a standard 'alpha prescription' (where we adopt $\alpha_{\rm CE}\lambda = 1$; see Iben & Livio 1993), but taking into account the initial positive energy. In particular, if this compact object is a neutron star, a compact binary containing a neutron star and a white dwarf is formed. We assume that, during the CE phase, the neutron star will accrete a significant amount of the envelope material and will become a millisecond pulsar (Bethe & Brown 1998). If the resulting mass of the neutron star exceeds the limit for a neutron star (taken in our simulations to be 2 $M_\odot$), we assume that a black hole is formed.

To evolve the cluster population of single stars and binaries in our code, we consider two basic time-scales. One is associated with the evolutionary changes in the stellar population, $\Delta t_{\rm ev}$, and the other with the rate of encounters, $\Delta t_{\rm coll}$ (see Section 3.4). The evolution time-step $\Delta t_{\rm ev}$ is computed so that no more than 2 per cent of all stars change their properties (mass and radius) by more than 5 per cent. The global time-step for the cluster evolution is taken to be $\Delta t = \min\,[t_{\rm ev}, t_{\rm dyn}]$.

3.3 Dynamical cluster model

As we described in Section 2, our model for the cluster dynamics is highly simplified. We adopt a simple two-zone, core–halo model for the cluster. We assume that the core number density, $n_{\rm c}$, and one-dimensional (1D) velocity dispersion, $\sigma_{\rm 1D}$, and the half-mass relaxation time, $t_{\rm rh}$, remain strictly constant throughout the evolution. While dense globular clusters of interest have $\sigma_{\rm 1D} \sim 10$ km s^{-1}, the core density can vary by several orders of magnitude. Here we set $n_{\rm c} = 10^5$ pc^{-3} for most calculations, representative of a fairly dense cluster such as 47 Tuc. In general, $n_{\rm c}$ is the main 'knob' that we can turn to increase or decrease the importance of dynamics. Setting $n_{\rm c} = 0$ corresponds to a traditional population synthesis simulation, where all binaries and single stars evolve in isolation after a single initial burst of star formation. To model a specific cluster, we match its core mass density today, $\rho_M^{\rm ob}$, central velocity dispersion and half-mass relaxation time.

The escape speed from the cluster core can be estimated from observations as $v_{\rm e} \simeq 2.5\,\sigma_{\rm 3D}$ (Webbink 1985), where $\sigma_{\rm 3D}$ is the three-dimensional (3D) central velocity dispersion. Following an interaction or a supernova explosion, any object that has acquired a recoil speed exceeding $v_{\rm e}$ is removed from the simulation. Acquiring a large recoil velocity in a dynamical encounter is a very efficient mechanism for ejecting low-mass objects from the cluster. We find generally that recoil to the halo does not play a significant role: the recoil velocity into the halo differs by $\sim$10 per cent from the escape velocity from the cluster, and affects only a small number of objects.

For computing interactions in the core, the velocities of all objects are assumed to be distributed according to a lowered Maxwellian (King 1965), with

$$f(v) = v^2/\sigma^2(m)\Big\{\exp[-1.5v^2/\sigma^2(m)] - \exp\Big[-1.5v_{\rm e}^2/\sigma^2(m)\Big]\Big\}, \quad (1)$$

where $\sigma(m) = (\langle m\rangle_{\rm c}/m)^{1/2}\sigma_{\rm 3D}$ (assuming energy equipartition in the core) and $v_{\rm e}$ is the escape speed. Here $\langle m\rangle_{\rm c}$ is the average mass of an object in the core. In addition, we use σ to impose a cut-off for soft binaries entering the core: any binary with maximum orbital speed $< 0.1\,\sigma_{\rm 3D}$ is immediately broken into two single stars (Hills 1990).

In the presence of a broad mass spectrum, the cluster core is always dominated by the most massive objects in the cluster, which tend to concentrate there via mass segregation. As stars evolve, the *composition* of the core will therefore change significantly over time. Mass segregation in globular clusters was investigated recently in Fregeau et al. (2002) by considering both light and heavy tracers in two-component models. It was found that the characteristic mass-segregation time-scale is given by

$$t_{\rm sc} \simeq 10\,C\,(\langle m\rangle_{\rm h}/m)\,t_{\rm rh}, \quad (2)$$

where C is a constant of the order of unity and $\langle m\rangle_{\rm h}$ is the average mass of an object in the halo, and m is the current mass of the object. This equation represents a diffusion process and can be applied to all stars, not just to those more massive than average. Indeed, even low-mass objects may (rarely) diffuse into the cluster core on a long time-scale, although on average they will tend to drift outwards. However, for very light objects with masses $\lesssim$0.4 $\langle m\rangle_{\rm h}$ (which is typically $\sim$0.3 $M_\odot$ at the beginning and $\sim$0.15 $M_\odot$ after $\sim$10 Gyr), this expression becomes less accurate, although it remains valid qualitatively. For a more recent discussion of mass segregation in the presence of a broad mass spectrum, see Gürkan, Freitag & Rasio (2004).

To model mass segregation in our simulations, we adopted the time-scale given by equation (2), but treated the process as stochastic: the probability for an object of mass m to enter the core after a time $t_{\rm s}$ is sampled from a Poisson distribution,

$$p(t_{\rm s}) = (1/t_{\rm sc})\exp(-t_{\rm s}/t_{\rm sc}). \quad (3)$$

This treatment ensures that all stars heavier than $\sim$0.4 $\langle m\rangle_{\rm h}$ diffusing into the core will have the appropriate mass spectrum and that interactions will occur between objects drawn from the correct distribution.

Equation (2) was derived for the restricted case of a two-component cluster – without a realistic IMF – therefore C is unknown by a factor of a few. We find in simulations that the final core mass is nearly proportional to $1/C\langle m\rangle_{\rm h}$. In order to obtain a better fit to observations for the core mass versus total cluster mass relation, we have fine-tuned equation (2) using data for 47 Tuc, in particular the ratio of the core mass to the total mass of the cluster. For this cluster we adopted a core mass of 10^5 $M_\odot$ and a total cluster mass of 10^6 $M_\odot$ at present (Freire et al. 2001); we also take $t_{\rm rh} = 3 \times 10^9$ yr (Harris 1996) and an age of 11 Gyr (Gratton et al. 2003). While the core mass can be found directly from our simulations, the total cluster mass has an uncertainty due to the IMF cut-off at the low-mass end in our standard cluster model. First, we found the total mass of a cluster model evolved to 11 Gyr and the initial number of very massive stars (defined as those producing a black hole at the end of their stellar evolution). We find that at 11 Gyr, the cluster has 145 $M_\odot$ per black hole (or per heavy primordial star), when the IMF extends down to 0.01 $M_\odot$. This allows us to normalize our model to the real cluster mass: with this ratio we have an estimate for the total cluster mass when we use a higher cut-off for the IMF (0.05 $M_\odot$). This now gives us the ratio of the core mass to the total cluster mass corresponding to our simulations. We find that the best fit for 47 Tuc gives $C\langle m\rangle_{\rm h} = 3\,M_\odot$.

3.4 Treatment of dynamical interactions

All objects in our simulations are allowed to have dynamical interactions only after they have entered the cluster core. We use a simple Monte Carlo prescription to decide which pair of objects actually have an interaction during each time-step.

The cross-section for an encounter between two objects, of masses m_i and m_J, with relative velocity at infinity v_{iJ}, is computed as

$$S_{iJ} = \pi d_{\max}^2 \left(1 + v_{\rm p}^2/v_{iJ}^2\right), \quad (4)$$

where $d_{\max}$ is the maximum distance of closest approach that defines a significant encounter and $v_{\rm p}^2 = 2G\,(m_i + m_j)/d_{\max}$ is the velocity at pericentre. Here the index i (lowercase) reflects an individual object in the core, while J (uppercase) denotes a random representative object from the *subclass* of objects J. In order to more accurately determine encounter rates, at each time-step binaries and single stars in the core are divided into 100 subclasses: 10 by size (radius for single stars or semimajor axis for binaries) and 10 by mass. Boundaries between mass subclasses are fixed approximately as 0.1×2^n. Subclasses by size depend on the current sizes of single and binary populations (separately), with the step between subclasses taken as $\delta \log_{10} r_{\rm bin} = 0.1\ (\log_{10} R_{\max} - \log_{10} R_{\min})$. The encounter rate for a given object i and an object from subclass J is $\Gamma_{i,J} = n_J S_{iJ} v_{iJ}$, where n_J is the number density of objects in subclass J, and the cross-section and relative velocity are defined for an average object in subclass J.

The total interaction rate for a given object i is the sum of the interaction rates with all relevant subclasses, $\Gamma_i = \sum_J n_J S_{iJ} v_{iJ}$. The corresponding interaction time is $\tau_i = 1/\Gamma_i$. The actual time for an encounter t_i follows a Poisson distribution with mean τ_i. In practice, we generate a random number $0 < X < 1$, and assume that the encounter happened if $t_i = X\tau_i \leqslant \Delta t$. The time-step is limited so that $\Delta t_{\rm dyn} \leqslant 0.25\ \min_i\ \tau_i$. We keep track separately of the time-scales $\tau_{i,J}$ for interactions with each subclass J, and the corresponding $t_{i,J} = X_J \tau_{i,J}$ is generated from an independent random number. If an encounter happened, it is assumed to be with an object from the subclass with the smallest $t_{i,J}$. The actual interacting object $\hat{J}$ from that subclass J is randomly selected from the list of non-interacted objects in this subclass.

In this paper we consider separately binary–binary, binary–single and single–single interactions. The cross-sections and rates are calculated using $d_{\max} = 5\,(R_i + \langle R\rangle_J)$ for single–single, $d_{\max} = 3\,(b_i + \langle R\rangle_J)$ for binary–single and $d_{\max} = 3\,(b_i + \langle b\rangle_J)$ for binary–binary. Here $b_i = a_i(1 + e_i)$ is the apocentre separation of the binary (a_i is the semimajor axis and e_i is the eccentricity), $\langle R\rangle_J$ is the average stellar radius in subclass J and $\langle b\rangle_J$ is the average apocentre separation in subclass J. A single–single interaction with pericentre distance $d_i \leqslant 2(R_i + R_J)$ is treated as a physical collision and assumed to lead to a merger or a dynamical CE phase. If $2 < d_i/(R_i + R_J) < 5$, we check whether a binary could be produced via tidal capture using the approach described in Portegies Zwart & Meinen (1993). If a tidal-capture binary is formed, its eccentricity is set to zero and its semimajor axis set to $2d_i$, assuming rapid circularization ($\sim$10 yr) as predicted by the standard model described in McMillan, McDermott & Taam (1987).

Each dynamical interaction involving a binary is calculated using FEWBODY, a new numerical toolkit for simulating small-N gravitational dynamics that provides automatic calculation termination and classification of outcomes (for a detailed description see Fregeau et al. 2004). FEWBODY numerically integrates the orbits of small-N systems, and performs collisions in the sticky-star approximation. The ability of FEWBODY to automatically classify and terminate calculations as soon as the outcome is unambiguous makes it well suited for carrying out large sets of binary interactions, for which calculations must be as computationally efficient as possible.

4 TEST CALCULATIONS AND SIMPLE ESTIMATES

4.1 Comparison with *N*-body simulations

We have compared our simple dynamical model to recent results from fully self-consistent Monte Carlo simulations based on Hénon's algorithm for solving the Fokker–Planck equation (Joshi, Rasio & Portegies Zwart 2000; Joshi, Nave & Rasio 2001). For our test we used the results obtained for an idealized model cluster containing 20 per cent primordial hard binaries (binding energies in the range 1–133 kT, where kT is the average kinetic energy of an object in the cluster) for a King model with dimensionless central potential $W_0 = 7$ (Fregeau et al. 2003, hereafter F03). In this simulation all stars had equal masses, were treated as point masses (no physical collisions), no stellar evolution was taken into account and all binary interactions were treated using simple recipes.

We used our code to perform a similar simulation: we considered a cluster consisting of equal-mass stars, and we turned off all stellar evolution and physical collisions. To fit the F03 model, we took the core mass as 8.3 per cent of the total cluster mass (corresponding to a King model with $W_0 = 7$), and we took an average star mass of 1 $M_\odot$ and $\sigma_{\rm r} = 10$ km s^{-1}. For a total cluster mass of 3×10^5 $M_\odot$ these conditions imply $t_{\rm rh} = 8 \times 10^8$ yr and $n_{\rm c} = 2000$ pc^{-3}. We evolved the cluster for $20\,t_{\rm rh}$.

In Fig. 1 we show our results for the core and halo binary fractions as a function of time, compared with the model of F03. The agreement with F03 is excellent: the core binary fraction rises very quickly to $\sim$35 per cent and then remains close to this value for $\sim 10\ t_{\rm rh}$. In contrast, the halo binary fraction decreases more

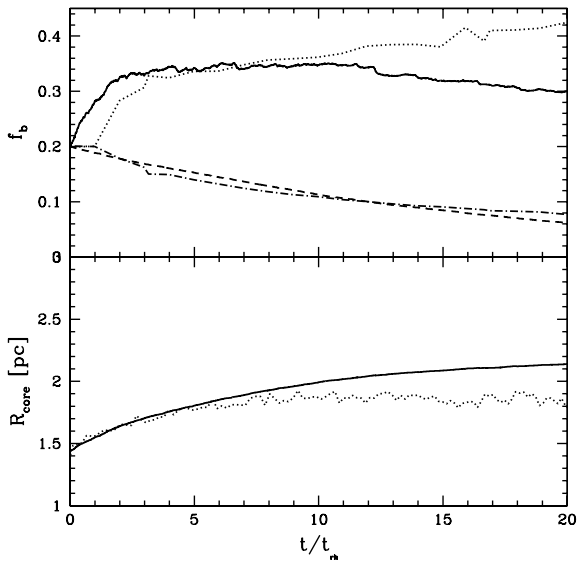

Figure 1. Evolution of the core and halo binary fractions (top) and the core radius (bottom) in our test model, compared with the F03 model (see the text). In the top panel, the solid line shows the binary fraction in the core and the dashed line shows the binary fraction in the halo, both for the test model. The dotted line shows the binary fraction in the core in the F03 model and the dash-dotted line shows the binary fraction in the halo in the F03 model. In the bottom panel the solid line shows the core radius in the test model and the dotted line shows the core radius in the F03 model.

gradually from 20 to 10 per cent. Considering the differences between the two treatments, especially for binary interactions, this agreement is quite remarkable.

In the bottom panel of Fig. 1 we show the evolution of the core radius r_c. The core radius evolves in the same way as in the dynamical simulation of F03. Overall, the core radius does not change much during the entire evolution and its value is consistent with the measured values for observed globular clusters with similar parameters (e.g. NGC 3201 or 6254, in which the total cluster mass, the central number density and the central velocity dispersion are similar to those in our model).

4.2 Semi-analytic estimates

One can estimate the final binary fraction $f_{\rm b,c}$ in a dense environment by considering several mechanisms of binary destruction.

(i) All soft binaries are usually destroyed during a strong encounter.

(ii) Some fraction of hard binaries is destroyed through stellar evolution (mergers or disruptions after supernova explosions).

(iii) When a hard binary has a strong encounter with another hard binary or a single star, it can exchange its less massive component for a more massive star, shrink its orbit or be destroyed in a collisional merger.

It should be noted that in our simplified semi-analytical treatment we neglect the effect of mass segregation, which tends to increase the core binary fraction. (This issue is discussed in more detail in Section 5.2.)

Let us consider a dense environment with number density 10^5 pc^{-3}, $\sigma_{\rm 1D} = 10$ km s^{-1} and with an average mass of 0.5 M$_\odot$. With our choices of initial parameters, and an average mass of 0.5 M$_\odot$, 40 per cent of all primordial binaries initially are soft (this fraction would be 50 per cent with respect to the average mass of 1 M$_\odot$). We introduce η – the hardness of a binary system – as

$$\eta = \frac{Gm_1m_2}{a\sigma^2\langle m\rangle}, \tag{5}$$

where a is the binary separation, m_1 and m_2 are the masses of the binary components and $\langle m\rangle$ is the average mass of a single star. Binaries that have $\eta < 1$ are termed soft, and those with $\eta > 1$ are termed hard.

To find how many hard binaries will be destroyed by stellar evolution alone, we calculated the probability of binary destruction as a function of its initial total mass and orbital period, using the binary population synthesis code (see Fig. 2). This simulation was performed with 1.25×10^5 binaries distributed initially flat in $\log P_{\rm d}$ and $\log M_{\rm tot}$ (in order to have better resolution for destruction rates for high-mass binaries), where $P_{\rm d}$ is the binary period in days and $M_{\rm tot} = M_1 + M_2$ is the total binary mass in M$_\odot$, and was evolved for 14 Gyr.

The result is striking: most of the very hard binaries, with hardness ratios $\eta \gtrsim 100$, are destroyed by stellar evolution. The empty space near the bottom right-hand corner of Fig. 2 reflects the absence of systems below the minimum period for binaries on the main sequence (the period at which stars come into contact). For binaries with total mass $\geqslant$10 M$_\odot$ destructions mainly occur during the first 10^8 yr of cluster evolution. Binaries with period $\geqslant 10^4$ d are mainly destroyed through SN explosions. Binaries with period $\leqslant$10 d are destroyed mainly via mergers at the MS stage. For periods in the range 10–10^4 d the destructions are associated with common envelope evolution and occur at later times. Destructions in binaries

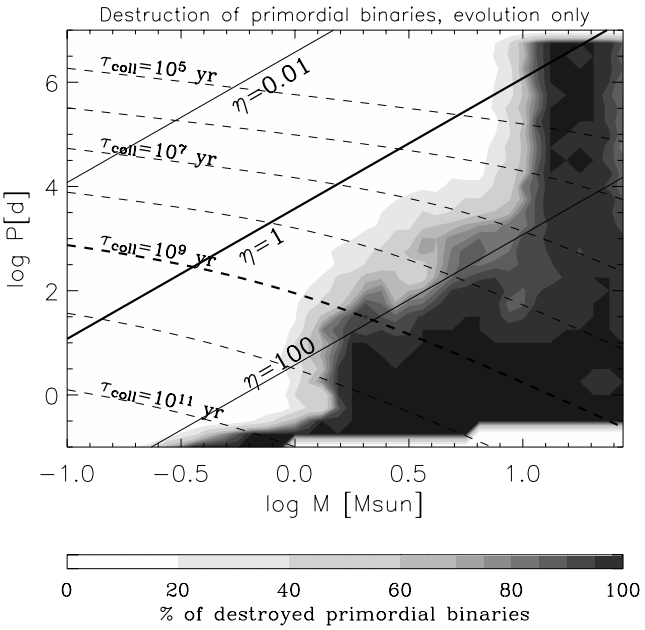

Figure 2. Destruction of primordial binaries by stellar evolution, shown in the parameter space of total initial binary mass and initial binary period. Solid lines are lines of constant binary hardness and dashed lines are lines of constant collision time.

of smaller masses are not much different from more massive binaries at small periods, but are not destroyed through SN explosions at large periods. Also, the CE event in less massive binaries occurs when the donor is a less evolved giant (at the first red giant branch).

One may expect that destruction rates should vary smoothly; however, binary evolution involves many qualitatively different events. In particular, an interesting fluctuation in destruction rates can be seen at $\log P \sim 1.75$ and $\log M_{\rm tot} \sim 0.95$, where local destruction rates are lower than for nearby binaries. For these and nearby binaries the destruction rates are approximately the same for mass ratio $q \lesssim 0.5$ but different for larger q. For binaries of masses close to and smaller than these, most destructions for $q \gtrsim 0.5$ occur during the CE event between a WD and a giant. This CE phase is the second interaction in the binary and follows the stable MT event with the other donor. When the total binary mass is smaller, the WD mass is $\lesssim$0.9 M$_\odot$, and a CE event leads to a merger. For binaries of higher total mass, the second interaction occurs between a He star or a WD and a star at the Hertzsprung gap. This MT is unstable and leads to a merger. This, therefore, provides for a small local decrease in destruction rates.

With our IMF and considering binaries of all masses, the fraction of hard binaries destroyed during their evolution is 20 per cent. Among binaries where at least one star is more massive than 0.5 M$_\odot$ the destruction fraction is 50 per cent, and for those with total initial mass above 1 M$_\odot$, this fraction is closer to 60 per cent. The fraction of hard binaries that is not destroyed but is instead softened by evolution is very small, $\leqslant$1 per cent. In Section 4.3 we will discuss in more detail how binary destruction rates change with time.

Therefore, even before any dynamical processes are considered for the hard binary population, we estimate that the final binary fraction cannot be higher than $\sim$50 per cent, and for binaries with at least one star more massive than 0.5 M$_\odot$ this upper limit becomes 30 per cent. For relatively massive binaries, with total initial mass above 1 M$_\odot$, the upper limit for $f_{\rm b,c}$ is only 24 per cent. Overall,

this estimate already shows that (i) the expected final binary fraction in a dense star cluster will be low and (ii) stellar evolution cannot be neglected when estimating binary fractions from dynamical models of dense star clusters.

Let us now consider the effects of dynamical interactions. The time-scale for a binary to undergo a strong encounter with another single star, the collision time, can be estimated as $\tau_{\rm coll} = 1/n\sigma v_\infty$. Assuming that the strong encounter occurs when the distance of closest approach $d_{\rm max} \leqslant ka$ with $k \simeq 2$, we obtain

$$\tau_{\rm coll} = 3.4 \times 10^{13}\ {\rm yr} \times k^{-2} P_{\rm d}^{-4/3} M_{\rm tot}^{-2/3} n_5^{-1} v_{10}^{-1} \times \left[1 + 913 \frac{(M_{\rm tot} + \langle M \rangle)}{k P_{\rm d}^{2/3} M_{\rm tot}^{1/3} v_{10}^2}\right]^{-1}. \quad (6)$$

Here $\langle M \rangle$ is the mass of an average single star in $M_\odot$, $v_{10} = v_\infty/(10\ {\rm km\ s^{-1}})$, where v_∞ is the relative velocity at infinity and $n_5 = n/(10^5\ {\rm pc^{-3}})$, where n is the number density. Using equation (5), equation (6) can be rewritten in a more convenient form:

$$\tau_{\rm coll} = 1.7 \times 10^8\ {\rm yr} \times \eta^2 k^{-2} n_5^{-1} \frac{\langle M \rangle^2}{M_1^2 M_2^2} \times \left(1 + \eta \frac{2}{k} \frac{M_{\rm tot} + \langle M \rangle}{M_1 M_2} \langle M \rangle\right)^{-1}. \quad (7)$$

It can be seen from equation (7) that the collision time for a binary with $\eta = 1$ and $M_{\rm tot} = 1\ M_\odot$ is only $\sim 10^8$ yr. Overall, with our IMF, $\sim$50 per cent of all hard binaries have collision times shorter than $\sim$10 Gyr (see also Fig. 2), and 15 per cent have collision times as short as $\sim$1 Gyr. In addition, most of the hard binaries that could have experienced an encounter are binaries with $\eta = 1$–100, and therefore they are from the population that is destroyed by stellar evolution to a lesser degree than binaries harder than $\eta = 100$. While this estimate considered only binary–single encounters, binary–binary encounters will further enhance the destruction rate. Moreover, when the binary fraction is higher than $\sim$25 per cent, binary–binary encounters dominate over binary–single encounters.

Each binary–single encounter with a hard binary can result in a hardening of this binary, an exchange of a companion with a more massive single star, or binary destruction in a physical collision. The probability of a physical collision during an encounter increases strongly as the binary becomes harder (Fregeau et al. 2004). In addition, a very hard binary can be ejected from the core if its recoil velocity exceeds the escape speed from the cluster. Each of these three processes, directly or indirectly, leads to the depletion of binaries (immediate or delayed): acquiring a more massive companion, and orbital shrinkage or the eccentricity increase, makes systems more likely be destroyed through stellar evolution. As a conservative lower limit, we assume that half of the interacting hard binaries will be destroyed as a result of an encounter (immediately or later). This is clearly a lower limit, as scattering experiments show that, for hard binaries containing main-sequence stars most encounters will lead to a physical collision (Fregeau et al. 2004).

Taking everything into account, we conclude that 64 per cent of all binaries will be destroyed – only $k_{\rm s} = 36$ per cent of primordial binaries can survive to the present. The expected final binary fraction is therefore $f_{\rm b} = N_{\rm b}/(N_{\rm s} + N_{\rm b}) = k_{\rm s}/(2 - k_{\rm s}) = 22$ per cent (for stars over the entire mass range) and it is 13 per cent ($k_{\rm s} = 23$ per cent) for binaries with at least one star more massive than 0.5 $M_\odot$, while for $M_{\rm tot} \geqslant 1\ M_\odot$ it is only 10 per cent ($k_{\rm s} = 18$ per cent). We note again that this upper limit for the final binary fraction does not take into account several other mechanisms leading to binary destruction, such as binary–binary encounters, which are more likely to cause binary destruction than binary–single encounters.

4.3 Encounters in dense environments

In order to verify our encounter rates, we considered the evolution of a binary population that is completely immersed into a dense environment with $n_{\rm c} = 10^5\ {\rm pc^{-3}}$ for its entire evolution. We adopted a velocity dispersion $\sigma_{\rm 1D} = 10\ {\rm km\ s^{-1}}$ and evolved the system for 14 Gyr. This is an even simpler model of a star cluster, where all objects are effectively inside the 'core' at all times and the effects of mass segregation and diffusion between a core and a halo are completely ignored. It allows us to study more clearly the various types of dynamical interactions as separate processes. We ran a sequence of simulations, with: (i) only binary–single encounters, with no physical collisions allowed during an encounter; (ii) binary–single encounters with physical collisions; (iii) both binary–single and binary–binary encounters but still without physical collisions; (iv) binary–single and binary–binary encounters with physical collisions; and (v) all types of encounters allowed, including single–single collisions. In this last case we also eliminated from the system any object that acquired a recoil speed exceeding the escape velocity $v_{\rm e} = 2.5\sigma_{\rm 3D}$.

In Section 4.2 we estimated that, with only binary–single encounters taken into account, the final binary fraction should not exceed 22 per cent. This assumed that all objects in the core had a mass equal to the average mass 0.5 $M_\odot$. With the complete IMF, a single star participating in the encounter can have mass higher than 0.5 $M_\odot$. Also, a fraction of initially hard binaries can become soft during the evolution, e.g. because of mass loss. As a result, we obtain even lower remaining binary fractions: $f_{\rm b,c} = 16.5$ per cent for case (i) and $f_{\rm b,c} = 16.4$ per cent for case (ii). These numbers are in agreement with the upper limits we estimated in Section 4.2.

When binary–binary encounters are taken into account, the result is even more dramatic: we obtain $f_{\rm b,c} = 8.0$ per cent and $f_{\rm b,c} = 7.9$ per cent for cases (iii) and (iv), respectively. As expected, we see that binary–binary encounters further enhance the binary destruction rate.

When all dynamical processes are taken into account, in case (v), we obtain a final binary fraction $f_{\rm b,c} = 6.9$ per cent. While our semi-analytical estimate of the binary fraction provided an upper limit, the result obtained in this section is clearly a lower limit: in a real cluster, not all binaries will be exposed to the high interaction rates of the core at all times. However, as more massive objects are more likely to diffuse into the core, and as their destruction rate can be higher than for objects of average mass, this lower limit is only approximate, but we may expect it to be much closer to the real value than our previous, conservative upper limit.

Let us now consider in detail which mechanisms of binary destruction are most important. In Fig. 3 we show the rates of binary destruction (events per binary per Gyr) for a field population (with no interactions). Except for the interval between $\sim 10^7$ and $\sim 10^8$ yr, when black holes and neutron stars are formed, the binary destructions are mainly coming from mergers. The power-law behaviour observed for the overall destruction rate at late times is on the one hand imposed by the rate of orbital decay driven by magnetic braking, and on the other hand depends on the evolutionary time-scale for the companion to become a red giant.

In Fig. 4 we show the binary destruction rates again, but for the dense environment. During the first few Gyr the main destruction mechanism is the dynamical disruption of soft binaries. The rate of disruption through stellar evolution is smaller than in the

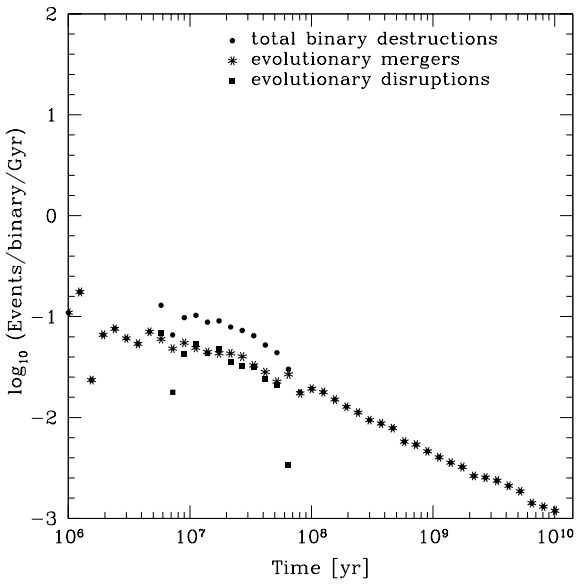

Figure 3. Binary destruction rates as a function of time for a field population (i.e. without dynamical interactions). Rates are given as numbers of events per binary per Gyr for mergers and disruptions (following a supernova explosion). Note the peak in evolutionary disruptions at $t \sim 10^7$–10^8 yr, which is due to supernovae.

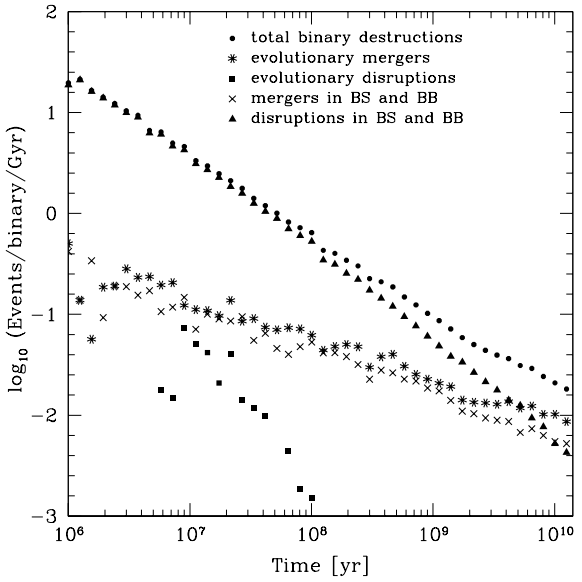

Figure 4. Same as in Fig. 3, but now for the same binary population evolved in a high-density environment with 10^5 binaries pc^{-3}. Here disruptions through binary–binary (BB) and binary–single (BS) interactions dominate for the first ∼5 Gyr.

field population: some massive binaries are destroyed by dynamical encounters before they evolve to a supernova explosion. However, the rate of evolutionary mergers is approximately the same as for the field for the first $\sim 10^8$ yr. This is consistent with our estimate for the collision time of hard binaries: at this time, hard binaries have not yet been hardened significantly by dynamical encounters. After $\sim 10^8$ yr the rate of binary evolutionary mergers is increased compared with the field population, as the dynamical hardening of hard binaries has now started. The rates for binary destruction through mergers and physical collisions are very similar: in most cases, if a binary is tight enough for an evolutionary merger, the most likely outcome of a dynamical interaction is a physical collision.

At ∼5 Gyr, the rate of binary destruction through physical collisions starts dominating over dynamical disruptions: at this stage, almost no soft binaries are left, and the hard binaries are more likely to lead to physical collisions during an encounter. Consider a binary with $\eta \sim 1$ at this stage. From equation (7) we can find that a collision time of 5 Gyr corresponds typically to binary components of 0.1 and 0.05 $M_\odot$ (assuming an average mass ratio of 0.5 and an average field mass as 0.5 $M_\odot$). This binary is clearly at the lowest-mass end of our IMF, and therefore by this time almost all soft binaries in the simulation have been destroyed. On the other hand, consider some more massive binary, which has evolved through approximately half of its main-sequence lifetime, and has component masses of 0.8 and 0.4 $M_\odot$ (and still the same collision time of 5 Gyr). The hardness of such a binary is $\eta \simeq 100$, corresponding to a binary separation $\simeq 10\,R_\odot$. For such a tight binary, the probability of a physical collision in an encounter is almost 100 per cent. The total rate of binary destructions through physical collisions become comparable to that of dynamical disruptions, as can be seen from Fig. 4.

5 RESULTS

5.1 Overview of cluster models

Initial conditions for all of our models are given in Table 1. The first group of models is used to cover the parameter space of initial conditions over fairly wide ranges. Our main reference model, model 1, has a core density of $n_c = 10^5$ pc^{-3}, a half-mass relaxation time of $t_{rh} = 10^9$ yr, an initial binary fraction of $f_{b,0} = 1$, a central velocity dispersion of $\sigma_{1D} = 10$ km s^{-1} and a central escape speed of $v_e = 2.5\,\sigma_{3D} = 43$ km s^{-1}. We then consider three models with different central densities (D3, D4 and D6), two with different half-mass relaxation time (T8 and T10) and one with an initial binary fraction decreased to 50 per cent (B05). The initial total number of stars is $N = 2.5 \times 10^5$ for all models, except for the '47 Tuc' model (see below), where we used $N = 5 \times 10^5$). In all of these models the cluster core was assumed to contain ∼1 per cent of the stars initially and the metallicity was fixed at $Z = 0.001$ (these two parameters have very little influence on our results).

Table 1. Initial conditions for all models.

Model	$\log n_c$	$\log \rho_M^{ob}$	$\log t_{rh}$	$f_{b,0}$	σ_{1D}	v_e
1	5.0		9.0	1.0	10.0	43.0
D3	3.0		9.0	1.0	10.0	43.0
D4	4.0		9.0	1.0	10.0	43.0
D6	6.0		9.0	1.0	10.0	43.0
T8	5.0		8.0	1.0	10.0	43.0
T10	5.0		10.0	1.0	10.0	43.0
B05	5.0		9.0	0.5	10.0	43.0
M12	3.8	3.5[a]	9.02	1.0	4.5	19.6
M4	4.4	4.1	8.82	1.0	4.2	20.3
47 Tuc	5.3	5.1	9.48	1.0	11.5	56.8
NGC 6388	5.9	5.7	9.08	1.0	18.9	78.2

Notation: n_c is the core number density in pc^{-3} (assumed fixed), ρ_M^{ob} is the observed core mass density in $M_\odot$ pc^{-3}, t_{rh} is the half-mass relaxation time in yr, $f_{b,0}$ is the initial binary fraction, σ_{1D} is the 1D velocity dispersion in km s^{-1} and v_e is the escape speed in km s^{-1}

[a] t_{rh} for specific clusters are taken from Harris (1996), ρ_M^{ob} and σ_{1D} from Pryor & Meylan (1993), and v_e from Webbink (1985).

Table 2. Results for reference models.

Model	log ρ_M	$f_{\rm b,c}$	$f_{0.5}$	$f_{\rm wd}$
1	4.7	0.095	0.15	0.080
D3	2.7	0.265	0.37	0.165
D4	3.7	0.170	0.25	0.115
D6	5.7	0.035	0.055	0.055
T8	4.5	0.11	0.13	0.085
T10	4.8	0.055	0.07	0.055
B05	4.7	0.072	0.010	0.055

Here ρ_M is the core mass density in $M_\odot$ pc^{-3}, $f_{\rm b,c}$ is the binary fraction in the core, $f_{0.5}$ is the binary fraction for non-degenerate stars more massive than 0.5 $M_\odot$ and $f_{\rm wd}$ is the binary fraction among white dwarfs. Values for all quantities are given at 14 Gyr.

We performed several simulations with parameters that attempt to match those of specific globular clusters in the Galaxy (the bottom part of Table 1). All of these clusters are classified observationally as 'non-core-collapsed', meaning that they are well fitted by standard King models. These are precisely the kinds of clusters that, theoretically, we expect to be in the 'binary burning' thermal equilibrium state. For this set, we tried to consider the maximum range of dynamical parameters, while concentrating on clusters at relatively small distances and/or very well studied observationally, so that current or future observations could test our predictions. For our most important model, 47 Tuc, we also considered additional models in which we varied the initial binary fraction or introduced a time-dependent core density (see Section 5.5). For all of our models of specific observed globular clusters, the central number density was chosen in order to provide (at the actual age of the cluster, ∼11–13 Gyr) the best fit to the observed mass density $\rho_M^{\rm ob}$ (Pryor & Meylan 1993). Metallicities for these models are taken from Harris (1996).

5.2 Main reference model

First, we present our results for a typical dense cluster, represented by model 1. With 100 per cent binaries initially, the final core binary fraction (at 14 Gyr), $f_{\rm b,c}$, is only 9.5 per cent. This is strikingly low, given that the cluster started with *all* stars in binaries, and that binaries should concentrate more into the core through mass segregation, but it is expected from our estimates in Section 4. Decreasing the initial binary fraction, $f_{\rm b,0}$, to a more reasonable (but still large) 50 per cent reduces $f_{\rm b,c}$ further to 7 per cent, as shown in model B05 (see Table 2). The dependence of $f_{\rm b,c}$ on $f_{\rm b,0}$ is not linear. This is mainly due to mass segregation: decreasing $f_{\rm b,0}$ also increases the ratio of mean binary mass to mean stellar mass in the cluster, thereby resulting in a higher concentration of binaries in the core.

The majority (∼75 per cent) of destroyed binaries were disrupted by close dynamical encounters (or, rarely, following a supernova explosion). Note that some binaries that are initially hard eventually become soft after undergoing significant mass loss due to stellar evolution. About 20 per cent of the destroyed binaries experienced mergers, typically after significant hardening through interactions. A few per cent of the binaries lost were actually not destroyed but instead were ejected from the cluster as a result of recoil in strong encounters. Tidal capture did not play a significant role: the total number of tidal-capture binaries formed during the cluster lifetime is less than 1 per cent of the final number of binaries in the core. The total core mass during most of the cluster evolution (the last $\sim 10\,t_{\rm rh}$) did not vary by more than a factor of 2.

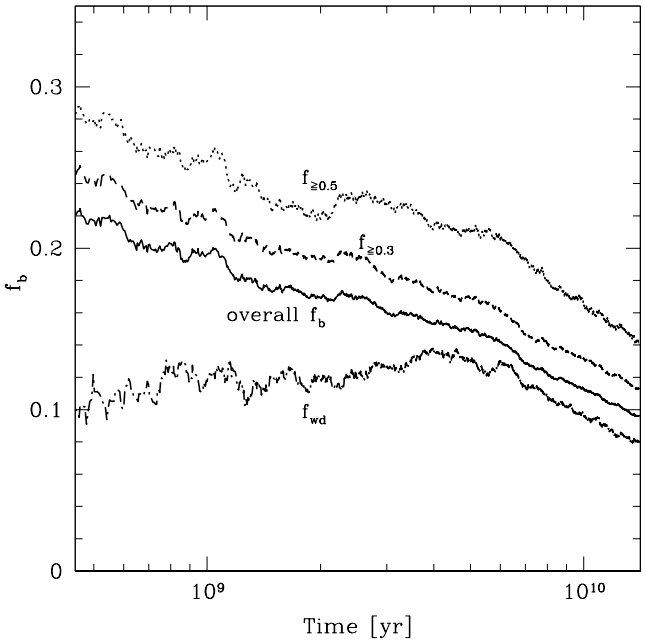

Figure 5. Evolution of the core binary fraction in model 1. We show separately the binary fractions for all objects, for non-degenerate stars with mass $\geqslant 0.5\,M_\odot$, for non-degenerate stars with mass $\leqslant 0.3\,M_\odot$ and for white dwarfs.

While the final core binary fraction is extremely low, the overall cluster binary fraction, which takes into account all halo binaries, remains high. However, the halo binaries consist mainly of very low-mass systems: the average primary mass among binaries remaining outside the core at 14 Gyr is 0.2 $M_\odot$, with the average companion mass being around 0.1 $M_\odot$. These binaries would be extremely faint and hard to detect observationally.

We have also examined different stellar subpopulations in the cluster: (i) the subpopulation of non-degenerate objects with mass (for a single star or for the primary in a binary) $\geqslant 0.5\,M_\odot$ and (ii) the subpopulation of all white dwarfs, single or in binaries. The binaries in group (i) may be easier to detect, e.g. from broadening of the main sequence in a colour–magnitude diagram (Rubenstein & Bailyn 1997). Binaries in group (i) are harder than less massive average binaries, so fewer of them are destroyed. On the other hand, stellar evolution plays a more significant role in the destruction of white-dwarf binaries, which were initially more massive and harder (Fig. 5). Therefore, the binary destruction rate in group (ii) is much higher, enhanced both by stellar evolution (mass loss and mass transfer at more advanced evolutionary stages, and supernovae in binaries), and by dynamical interactions (larger cross-section for encounters). Note also that the overall $f_{\rm b,c}$ is decreased partially through a lower binary fraction for degenerate objects.

5.3 Different densities and relaxation times

Let us now compare results for different central densities, in models 1, D3, D4 and D6. The evolution of $f_{\rm b,c}$ for these models is shown in Fig. 6. As expected, the core binary fraction decreases as $n_{\rm c}$ increases. The dependence is steeper at high densities, where dynamical interaction rates play a more dominant role compared with stellar evolution.

With respect to the half-mass relaxation time (models T8 and T10), we find that, surprisingly, the model with shorter relaxation time has a higher core binary fraction. There are two competing

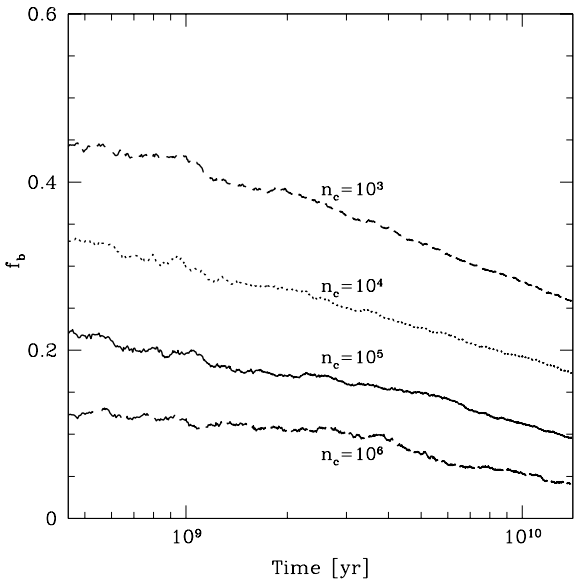

Figure 6. Evolution of the core binary fraction in model 1 compared with models with different core number densities (D3, D4 and D6).

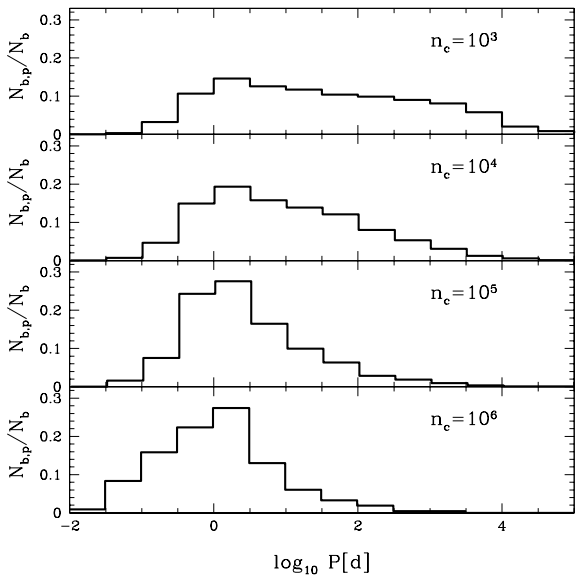

Figure 7. The binary period distributions in models with different densities (from the top: D3, D4, model 1 and D6). N_b is the total number of binaries and $N_{b,p}$ is the number of binaries in each period bin.

mechanisms that play a role here: mass segregation, which brings binaries into the core, and dynamical interactions, which destroy binaries in the core. A shorter segregation time increases the rate at which binaries enter the core but also allows less massive binaries to interact. Therefore, the average mass of a binary in the core and the effective mass density in the core are smaller. As a result, fewer binaries are destroyed.

5.4 Binary period distribution

Through dynamical interactions, we would expect that the initial period distribution of binaries should be depleted above the boundary between hard and soft binaries. Stellar evolution should deplete a fraction of hard binaries, especially at very short periods, and dynamical encounters should further deplete some of the wider hard binaries. Indeed, for lower-density clusters, we find that the distribution remains much flatter in log P (see Figs 8 and 9), with more and more of the wider hard binaries disappearing as the density increases.

This period distribution can be used to better extrapolate the observed binary fractions, which are usually limited to rather narrow ranges of masses and periods. In particular, it is clear that the usual assumption of a flat distribution in log P for hard binaries *at present* in a cluster core (e.g. Albrow et al. 2001) can be very misleading. This will be shown in Section 5.5 for our models of several real clusters.

5.5 Comparison with observations

We performed several simulations with parameters that attempt to match those of specific globular clusters in the Galaxy (Tables 1 and 3). For these models, the total core masses we compute at present match well those of King models fitted to the observed cluster parameters, and the corresponding core radii of our models (from total core mass and density) are all ∼0.5 pc, matching the observed values. In all cases the initial binary fraction is assumed to be 100 per cent, so our results for final core binary fractions represent upper limits. As in all reference models, we predict low values for $f_{b,c}$ in all globular clusters, with smaller values in higher-density cores.

We compare our derived binary fraction for M4 with the results

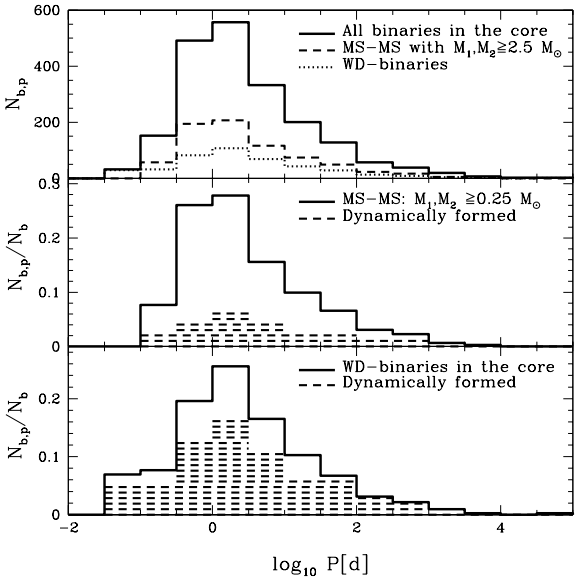

Figure 8. Period distributions for different binaries in model 1 (at 14 Gyr). The middle plot shows the period distribution of binaries containing two MS stars with masses greater than 0.25 $M_\odot$, bottom plot shows the period distribution of binaries with at least one WD; the shaded area shows the fraction of dynamically formed binaries. N_b is the total number of binaries and $N_{b,p}$ is the number of binaries in each period bin.

from Cote & Fischer (1996). Using a Monte Carlo modelling of the binary population, they found that the best fit to the observed binaries (in the period range from 2 d to 3 yr) is $f_{b,c} \simeq 15$ per cent. This is in good agreement with our overall predicted $f_{b,c} = 11.5$ per cent, and also with our prediction for heavier main-sequence binaries, $f_{0.5} = 17.5$ per cent.

In the 47 Tuc model (for which we increased the total number of stars initially to a more realistic $N = 5 \times 10^5$), $f_{b,c}$ is only 8 per cent at an age of 11 Gyr and ∼ 7 per cent at 14 Gyr (we provide this value at different ages given the uncertainty in observationally

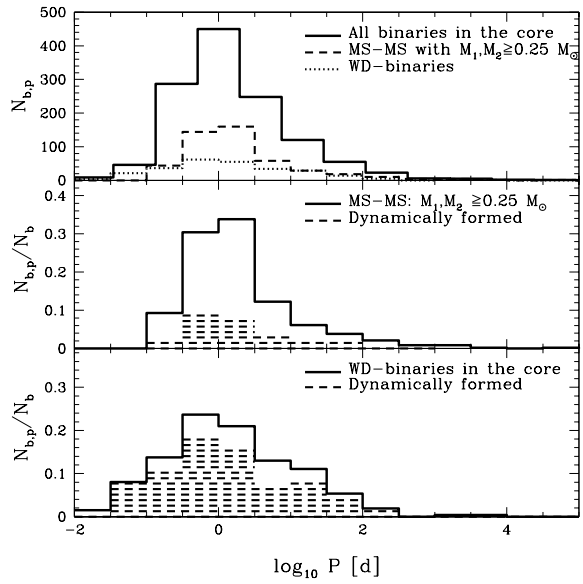

Figure 9. The binary period distribution in our 47 Tuc model, at 11 Gyr. The middle plot shows the period distribution of binaries containing two main-sequence stars with masses greater than 0.25 $M_\odot$; the bottom plot shows the period distribution of binaries with at least one white-dwarf component (the shaded area shows the fraction of dynamically formed binaries). As before N_b is the total number of binaries and $N_{b,p}$ is the number of binaries in each period bin.

Table 3. Results for models of specific clusters.

Model	Age	log ρ_M	$f_{b,c}$	$f_{0.5}$	f_{wd}
M12	12	3.5	0.170	0.26	0.130
M4	13	4.4	0.115	0.175	0.10
47 Tuc	11	5.1	0.080	0.125	0.075
NGC 6388	12	5.7	0.06	0.08	0.045

With the same notation as before, the columns give: the name of the cluster; the cluster age in Gyr; the central mass density in $M_\odot$ pc^{-3} in simulations at the given age, the core binary fraction, the binary fraction for non-degenerate objects more massive than 0.5 $M_\odot$ and the binary fraction among white dwarfs.

determined values for the ages of 47 Tuc; see, e.g., Schiavon et al. 2002; Zoccali at al. 2001; also note that $f_{b,c}$ does not change much over the last several Gyr). At first glance, this may seem to conflict with observations. In particular, Albrow et al. (2001) derive an overall binary fraction for the core of 47 Tuc of ∼13 per cent, from observations of eclipsing binaries with periods in the range $P \simeq$ 4–16 d. This estimate was based on an extrapolation assuming a flat period distribution that is in log P from ∼2.5 d to 50 yr (soft primordial binaries with $P > 50$ yr are assumed destroyed and short-period primordial binaries with $P \leqslant 4$ d are assumed to evolve toward much shorter periods through angular momentum loss by magnetic braking). In Fig. 9 we show the final period distribution of core binaries in our simulation. Note that the period range of eclipsing binaries is near the peak of the distribution, while for longer periods the number of binaries drops rapidly. In particular, if we concentrate on the binaries consistent with the observed set, with primary masses $M_1 > 0.25\,M_\odot$ and $q > 0.3$, we find that the number of systems with periods in the range 16 d–50 yr is approximately six times smaller than would be predicted by adopting a flat distribution that was in log P. For the whole period range from 2.5 d to 50 yr we have 2.2 times fewer binary systems compared with the flat distribution. If we take into account this depletion of wider binaries when modelling the number of observed eclipsing binaries in 47 Tuc, we are led to revise the observed core binary fraction from Albrow et al. (2001) to 6 ± 2 per cent, which is much closer to our theoretical prediction.

We performed three additional simulations for 47 Tuc, with $f_{b,0} = 0.25$, 0.5 and 0.75. The corresponding core binary fraction extrapolated from observations (corrected as above) does not vary much among these different models. Its maximum value is obtained for $f_{b,0} = 0.5$, which gives a core binary fraction of ∼ 8 per cent, and in this case the total number of binary systems is 1.6 times less than with an assumed flat distribution.

An alternative estimate of the binary fraction in the core of 47 Tuc is based on observations of BY Dra stars (Albrow et al. 2001). Their estimated core binary fraction, which can be considered a *lower limit*, is ∼0.8 per cent, 18 times lower than the estimate based on eclipsing binaries. This estimate was based on 31 BY Dra binaries (observed in the period range 0.4–10 d) and five eclipsing binaries (period range 4–16 d). We analysed the core binary population in our model in order to identify BY Dra systems and eclipsing binaries, and considering the ratio of the two. We adopted the standard definition for a BY Dra binary: primary mass in the range 0.3–0.7 $M_\odot$ (see, e.g., Bopp & Fekel 1977) and period in the range 0.4–10 d (as for the observed sample in 47 Tuc). For eclipsing binaries we adopted the observed period range 4–16 d with each star $\geqslant$0.25 $M_\odot$. The ratio between the number of BY Dra systems and the number of eclipsing binaries is found to be 5.9, 6.7, 7.2 and 3.5 for models with $f_{b,0} = 1.0$, 0.75, 0.5 and 0.25, respectively. Therefore, a large initial binary fraction $\gtrsim$75 per cent is most likely.

Of the quantities that we explicitly assume in our cluster model to be constant, the central (core) density is that with the largest dynamic range in models that provide for dynamical evolution. Hence it is also the quantity that is most likely to significantly affect our final results. To test the sensitivity of our results to a changing central density, we have run our model of 47 Tuc with a central density assumed to increase by a factor of 10 from $t = 0$ to the present. Specifically, we still match the currently observed core density while ramping up the value either exponentially or linearly in time, starting with a value 10 times smaller than at present. This could represent qualitatively the gradual core contraction observed in some N-body models of star clusters with binaries (see Aarseth & Heggie 1993, and, for a steeper core contraction, see Giersz & Spurzem 2003). These models predict a present-day core binary fraction that is only slightly higher, by ∼1–2 per cent. To increase the binary fraction more significantly, the time-averaged core density in the cluster would have had to be many orders of magnitude lower than what is observed today. There is no reasonable dynamical history that would produce such an unusual result. In contrast, recent N-body simulations show that the presence of just 10 per cent hard primordial binaries leads to core radius *expansion* and therefore the core density might be higher in the past (Wilkinson et al. 2003). Though we did not run another 47 Tuc model with a central density decreasing with time, we can predict that the present-day binary fraction would then be smaller by ∼1–2 per cent.

6 CONCLUSIONS

We have considered in detail processes of binary destruction (and formation) in dense stellar systems. In particular, we have shown that the present binary fraction in cluster cores should be relatively small

($\lesssim$10 per cent). This is caused not only by dynamical encounters, but also binary stellar evolution, which is the dominant mechanism for the destruction of hard binaries. We also find that the destruction rate due to stellar evolution is enhanced significantly by dynamical hardening of binaries.

We have shown that values of binary fractions for stars in different mass ranges and at different evolutionary stages can differ significantly. The fraction of dynamically formed binaries is higher when one considers stars at more advanced evolutionary stages. The binary period distribution evolves from flat in log P for loose clusters toward a sharply peaked distribution in denser clusters, even if all clusters have identical velocity dispersions and therefore identical hard–soft binary boundaries. This implies that a flat period distribution should not be assumed when deriving overall binary fractions by extrapolation from the distribution of observed binaries in a narrow period range (e.g. eclipsing binaries).

We considered several models that attempted to match observed globular clusters. For those with good available data on binaries (M4 and 47 Tuc), we found our predicted binary fractions to be in good agreement with observations once we take into account the correct binary period distribution. The main conclusion we derive from these calculations and our semi-analytic estimates is that the currently observed binary fractions in cluster cores suggest very high initial (primordial) binary fractions – close to 100 per cent.

In addition to their implications for the interpretation of observed binary fractions in cluster cores, our results have important consequences for the theoretical modelling of globular clusters using N-body simulations. Indeed, it is clear that 'realistic' dynamical simulations of globular cluster evolution should include large populations of primordial binaries, with initial binary fractions in the range $\sim$50–100 per cent (similar to what is usually assumed for the field; see, e.g., Duquennoy & Mayor 1991). This poses a particular challenge for direct N-body simulations, where the treatment of even relatively small numbers of binaries can add enormous computational costs. For this reason, current direct N-body simulations of star clusters with large initial binary fractions typically have N too small to be considered representative of globular clusters (see, e.g., Wilkinson et al. 2003; Portegies Zwart et al. 2004). Other methods, such as Monte Carlo simulations, do not suffer from the same limitations, and routinely simulate clusters with reasonably large N ($\sim 10^5$–10^6) and binary fractions ($\sim$30 per cent), but have not yet included advanced treatments of binary star evolution (see, e.g., Fregeau et al. 2003, and references therein).

ACKNOWLEDGMENTS

We thank D. Heggie and J. Hurley for very helpful discussions. This work was supported by NSF Grant AST-0206276, NASA ATP Grant NAG5-12044 and a *Chandra* Theory grant.

REFERENCES

Aarseth S. J., 2001, New Astron., 6, 277
Aarseth S. J., Heggie D. C., 1993, ASP Conf. Ser. Vol. 48, The Globular Cluster-Galaxy Connection, Astron. Soc. Pac., San Francisco, p. 701
Albrow M. D., Gilliland R. L., Brown T. M., Edmonds P. D., Guhathakurta P., Sarajedini A., 2001, ApJ, 559, 1060
Bacon D., Sigurdsson S., Davies M. B., 1996, MNRAS, 281, 830
Belczynski K., Kalogera V., Bulik T., 2002, ApJ, 572, 407
Bellazzini M., Fusi Pecci F., Messineo M., Monaco L., Rood R. T., 2002a, AJ, 123, 1509
Bellazzini M., Fusi Pecci F., Montegriffo P., Messineo M., Monaco L., Rood R. T., 2002b, AJ, 123, 2541
Benacquista M., 2002, Living Rev. Relat., 5, 2
Bethe H. A., Brown G. E., 1998, ApJ, 506, 780
Binney J., Tremaine S., 1987, Galactic Dynamics. Princeton Univ. Press Princeton, p. 747
Bopp B. W., Fekel F., 1977, AJ, 82, 490
Brandner W., Alcala J. M., Kunkel M., Moneti A., Zinnecker H., 1996, A&A, 307, 121
Chernoff D. F., Huang X., 1996, in Proc. IAU Symp. 174, Dynamical Evolution of Star Clusters: Confrontation of Theory and Observations. Astron. Soc. Pac., San Francisco, p. 263
Cool A. M., Bolton A. S., 2002, in ASP Conf. Ser. 263, Stellar Collisions, Mergers and their Consequences. Astron. Soc. Pac., San Francisco, p. 163
Cote P., Fischer P., 1996, AJ, 112, 565
Cote P., Pryor C., McClure R. D., Fletcher J. M., Hesser J. E., 1996, AJ, 112, 574
Davies M. B., 1995, MNRAS, 276, 887
Davies M. B., 1997, MNRAS, 288, 117
Davies M. B., Benz W., 1995, MNRAS, 276, 876
Di Stefano R., Rappaport S., 1994, ApJ, 437, 733
Dubath P., Meylan G., Mayor M., 1997, A&A, 324, 505
Duquennoy A., Mayor M., 1991, A&A, 248, 485
Freire P. C., Camilo F., Lorimer D. R., Lyne A. G., Manchester R. N., D'Amico N., 2001, MNRAS, 326, 901
Fregeau J. M., Joshi K. J., Portegies Zwart S. F., Rasio F. A., 2002, ApJ, 570, 171
Fregeau J. M., Gürkan M. A., Joshi K. J., Rasio F. A., 2003, ApJ, 593, 772 (F03)
Fregeau J. M., Cheung P., Portegies Zwart S. F., Rasio F. A., 2004, MNARS, 352, 1
Fryer C. L., Kalogera V., 2001, ApJ, 554, 548
Gao B., Goodman J., Cohn H., Murphy B., 1991, ApJ, 370, 567
Giersz M., Spurzem R., 2003, MNRAS, 343, 781
Goodman J., Hut P., 1989, Nat, 339, 40
Gratton R. G., Bragaglia A., Carretta E., Clementini G., Desidera S., Grundahl F., Lucatello S., 2003, A&A, 408, 529
Gürkan M. A., Freitag M., Rasio F. A., 2004, ApJ, 604, 632
Halbwachs J. L., Mayor M., Udry S., Arenou F., 2003, A&A, 397, 159
Harris W. E., 1996, AJ, 112, 1487
Heggie D. C., 1974, Celestial Mech., 10, 217
Hills J. G., 1984, AJ, 89, 1811
Hills J. G., 1990, AJ, 99, 979
Hurley J. R., Shara M. M., 2003, ApJ, 589, 179
Hurley J. R., Pols O. R., Tout C. A., 2000, MNRAS, 315, 543
Hurley J. R., Tout C. A., Pols O. R., 2002, MNRAS, 329, 897
Hut P., McMillan S., Romani R. W., 1992, ApJ, 389, 527
Iben I. J., Livio M., 1993, PASP, 105, 1373
Ivanova N., Taam R. E., 2003, ApJ, 599, 516
Ivanova N., Rasio F., 2004, Rev. Mex. Astron. Astrofis. Conf. Ser., 20, 67
Ivanova N., Rasio F., 2005, in Rasio F. A., Stairs I. H., eds, in ASP Conf. Ser. Vol. 238, Binary Radio Pulsars. Astron. Soc. Pac., San Francisco, p. 231 (astro-ph/0405382)
Joshi K. J., Rasio F. A., Portegies Zwart S., 2000, ApJ, 540, 969
Joshi K. J., Nave C. P., Rasio F. A., 2001, ApJ, 550, 691
King I. R., 1965, AJ, 70, 376
Köhler R., Leinert C., Zinnecker H., 2001, Astron. Gesellschaft Meeting Abstracts, 18, 24
Kroupa P., 2002, Sci, 295, 82
McMillan S. L. W., McDermott P. N., Taam R. E., 1987, ApJ, 318, 261
Melo C. H. F., 2003, A&A, 410, 269
Mikkola S., 1983, MNRAS, 203, 1107
Mikkola S., 1985, MNRAS, 215, 171
Portegies Zwart S. F., Meinen A. T., 1993, A&A, 280, 174
Portegies Zwart S. F., Hut P., McMillan S. L. W., Verbunt F., 1997a, A&A, 328, 130

Portegies Zwart S. F., Hut P., McMillan S. L. W., Verbunt F., 1997b, A&A, 328, 143
Portegies Zwart S. F., McMillan S. L. W., Hut P., Makino J., 2001, MNRAS, 321, 199
Portegies Zwart S. F., Hut P., McMillan S. L. W., Makino J., 2004, MNRAS, 351, 473
Pryor C., Meylan G., 1993, in ASP Conf. Ser. Vol. 50, Structure and Dynamics of Globular Clusters. Astron. Soc. Pac., San Francisco, p. 357
Rasio F. A., Pfahl E. D., Rappaport S., 2000, ApJ, 532, L47
Rubenstein E. P., Bailyn C. D., 1997, ApJ, 474, 701
Schiavon R. P., Faber S. M., Rose J. A., Castilho B. V., 2002, ApJ, 580, 873
Sigurdsson S., Phinney E. S., 1995, ApJS, 99, 609
Sills A. et al., 2003, New Astron., 8, 605
Shara M. M., Hurley J. R., 2002, ApJ, 571, 830
Smith K. W., Bonnell I. A., 2001, MNRAS, 322, L1
Tokovinin A. A., 1997, Astron. Lett., 23, 727
Verbunt F., Zwaan C., 1981, A&A, 100, L7
Webbink R. F., 1985, in IAU Symp. 113, Dynamics of Star Clusters. Reidel, Dordrecht, p. 541
Wilkinson M. I., Hurley J. R., Mackey A. D., Gilmore G. F., Tout C. A., 2003, MNRAS, 343, 1025
Woitas J., Leinert C., Köhler R., 2001, A&A, 376, 982
Zoccali M. et al., 2001, ApJ, 553, 733

APPENDIX: ROLE OF THREE-BODY BINARY FORMATION

Consider the rate of three-body binary formation (via the close approach of three single stars) in a dense cluster core. We denote by $\Gamma(E_{\rm b})$ the rate per star of the formation of a binary with binding energy $E_{\rm b}$. First, we consider $\Gamma(b \leqslant b_{\rm max})$ – the rate (per star) at which three objects come together within a region of size $b_{\rm max}$. The probability that a third object will be in the vicinity b of two other interacting objects is the product of the probability of the first two bodies meeting and the probability that during this time a third object will be in the same vicinity. The rate of two-body encounters for masses m_1 and m_2, with number density n_2 is

$$\Gamma_2(b \leqslant b_{\rm max}) = \pi b_{\rm max}^2 \left(1 + \frac{v_{\rm p}^2}{\langle v_{12}\rangle^2}\right) n_2 v_{12}, \tag{A1}$$

where

$$v_{\rm p}^2 = \frac{2G(m_1+m_2)}{b_{\rm max}} \tag{A2}$$

is the velocity at closest approach and

$$\langle v_{12}\rangle^2 \simeq \left(\sigma_1^2 + \sigma_2^2\right) = \sigma^2\langle m\rangle \frac{m_1+m_2}{m_1 m_2}, \tag{A3}$$

where σ is the three-dimensional velocity dispersion.

We define the minimum hardness for the binary to be formed as

$$\eta_{\rm min} = \frac{G m_1 m_2}{b_{\rm max}\langle m\rangle\sigma^2}. \tag{A4}$$

Then

$$\Gamma_2(b \leqslant b_{\rm max}) = \pi b_{\rm max}^2 (1+2\eta)\, n_2 v_{12}. \tag{A5}$$

The second object spends in the vicinity b of the first object a time $\Delta t \simeq 2\, b/v_{\rm p}$. The probability that a third object will be within the same vicinity is then

$$p_3 \simeq n_3\left(b_{\rm max}^2 \Delta t v_3 + b_{\rm max}^3\right) = n_3 b_{\rm max}^3 \left(1 + 2\frac{v_3}{v_{\rm p}}\right), \tag{A6}$$

where v_3 is the relative velocity of the third object with respect to the centre of mass of the first two. Effectively, it reflects velocity at which the population at the vicinity b is increasing. We do not consider here the population decrease, assuming that if the object was in the neighbourhood, a three-body encounter has happened.

The final result then takes the form given in Binney & Tremaine (1987, Section 8), but with an additional mass- and hardness-dependent factor f,

$$\Gamma_3(\eta > \eta_{\rm min}) = \frac{n_{\rm c}^2 G^5 \langle m\rangle^5}{\sigma^9} f(m_1, m_2, m_3, \eta) \tag{A7}$$

$$f(m_1, m_2, m_3, \eta) = \pi \frac{n_2 n_3}{n_{\rm c}^2} \frac{m_1^5}{\langle m\rangle^5} \frac{m_2^5}{\langle m\rangle^5} \eta^{-5} (1+2\eta) \times \left[1 + \frac{v_3}{\sigma}\eta^{-1/2}\sqrt{2\frac{m_1 m_2}{(m_1+m_2)\langle m\rangle}}\right] \frac{v_{12}}{\sigma}. \tag{A8}$$

It is clear that the rate is highly dependent on the masses of the participating stars and decreases steeply with increasing hardness of the binary that is formed.

If all encounters resulted in the formation of a binary with hardness η, then the rate of binary formation would be completely described by equation (A7).

Using the equation (A7), the time-scale for three-body binary formation can also be written as

$$T_{3b} = 2.08 \times 10^{16}({\rm yr}) \left(\frac{10^5}{n_{\rm c}}\right)^2 \left(\frac{{\rm M}_\odot}{\langle m\rangle}\right)^5 \left(\frac{\sigma}{10\ {\rm kms}^{-1}}\right)^9 \times \frac{n_{\rm c}}{n_2}\frac{n_{\rm c}}{n_3}\left(\frac{\langle m\rangle}{m_1}\right)^5 \left(\frac{\langle m\rangle}{m_2}\right)^5 \frac{\sigma}{v_{12}} \times \eta^5 (1+2\eta)^{-1} \left[1 + \frac{v_3}{\sigma}\eta^{-1/2}\sqrt{2\frac{m_1 m_2}{(m_1+m_2)\langle m\rangle}}\right]^{-1}. \tag{A9}$$

Even in the core of a large, very dense cluster, with density $\sim 10^5$ pc^{-3} and containing $\sim 10^5$ stars, no binaries with $\eta > 1$ will be formed from ~ 1 M$_\odot$ stars in a Hubble time. It has also been shown that many three-body binary formation events will lead to physical collisions for stars as small as white dwarfs (Chernoff & Huang 1996). We therefore neglect all three-body interactions in our cluster simulations.

This paper has been typeset from a TEX/LATEX file prepared by the author.